DETECTION OF LOW-LATITUDE PLUMES IN THE OUTER CORONA BY ULYSSES RADIO RANGING MEASUREMENTS

Richard Woo
Jet Propulsion Laboratory, California Institute of Technology, 4800 Oak Grove Drive, MS 238-725, Pasadena,CA91109

Michael K. Bird
Radioastronomisches Institut, Universität Bonn, Auf dem Hügel 71, 53121, Bonn, Germany

Martin Pätzold
Institut fur Geophysik and Meteorologie, Universität zu Köln, Germany

ABSTRACT

Plumes have been detected beyond the field of view of coronagraphs in the range of 23-42 R. in an equatorial coronal hole by Ulysses radio ranging measurements conducted in 1991 at 13 and 3.6 cm wavelengths. Exploiting the ranging measurement features of high sensitivity, wide dynamic range, high precision, high stability, and long duration, the plumes have been identified by the similarity in their path-integrated density profiles with those of polar plumes observed in white-light measurements of the inner corona. Like the polar plumes, the low-latitude plumes are consistent with radial expansion, and show a variation in path-integrated density of ±10%. These results show that plumes arc not exclusive to polar regions, but appear to be intrinsic to open magnetic field regions at any latitude.

1, INTRODUCTION

First captured on film during solar eclipses as early as a century ago [see for instance photograph by T.W. Smillie in Abbot (1900)], polar plumes have been the subject of considerable study (van de Hulst 1950; Saito 1965; Newkirk & Harvey 1968). Especially prevalent during the low activity portion of the solar cycle, polar plumes appear as faint but striking rays in polar coronal holes, presumably tracing the coronal magnetic fields. In addition to white-light (Koutchmy 1977; Koutchmy et al. 1994; Fisher & Guhuthakurta 1995), polar plumes have also been observed in soft X-ray (Ahmad and Webb 1978) and EUV (Bohlin, Sheeley, & Tousey 1974; Ahmad & Withbroe 1977; Widing & Feldman 1992; Walker et al. 1993) images. As one of the few observed features in coronal holes, plumes may very well have important implications for heating processes in the source region of the solar wind (Habbal 1992; Wang 1994; Velli, Habbal & Esser 1994; Habbal et al. 1995).

The emerging picture of a highly structured corona (Woo 1996a) — with a wide range of raylike structures starting with large-scale sizes such as streamers and extending down to sizes as small as 1 km at the Sun —- has spurred further exploration of these structures using radio propagation measurements. Carried out with natural or artificial radio sources passing behind the Sun as viewed from Earth, radio propagation measurements bridge the gap between solar observations and in situ plasma measurements made by spacecraft beyond 0.3 AU. Of the diverse radio propagation measurements, ranging and white-light are the most alike, since both observe path-integrated density off the limb of the Sun, and considerable progress has been made in understanding how these measurements complement each other (Woo et al. 1995a; Woo 1 996b). In this paper, large- and small-scale structures refer to the relative sizes as observed by radio propagation rather than white-light measurements. Although earlier investigations of the corona based on ranging measurements with spacecraft radio signals concentrated on the dominant radial variation of path-integrated electron density (Bird and Edenhofer 1990), recent work has demonstrated

that ranging measurements also contain information on the variation across the structured corona (Woo et al. 1995; Woo 1996c). Since the density variation across smaller structures represents only a small percentage of that across the large-scale structures, prominent features such as streamers readily appear in measurements that observe path-integrated density (ranging), while small-scale structure only in measurements that detect changes in path-integrated density (scattering and scintillation) (Woo 1996b). For the same reason, streamers and plumes dominate the images of white-light measurements of polarized brightness, with smaller structures becoming more discernible when the images have been processed to enhance density gradients (Koutchmy 1977; Guhathakurta and Fisher 1995; Woo et al. 1995; Woo 1996b). Thus, it might be expected that plumes would also be detected in ranging measurements.

In this paper, we present the first evidence for plumes in ranging measurements. The detection of plumes in the outer corona by ranging measurements complements the imaging measurements of white-light by providing evidence not only for the extension of plumes beyond the field of view of coronagraphs, but also their existence in low-latitude coronal holes. This paper is organized as follows. The Ulysses ranging measurements arc described in Section 2. The identification of plumes is discussed in Section 3, and conclusions are presented in Section 4.

2. ULYSSES RANGING MEASUREMENTS

The S- and X-band (13 and 3.6 cm wavelengths) ranging or time delay measurements, which observe path-integrated electron density (Bird and Edenhofer 1990) and arc analyzed here, were carried out during the 1991 solar conjunction of Ulysses, and belong to the same group of radio propagation measurements that have been used in earlier investigations of electron density (Bird et al. 1994), fractional density variations (Woo et al. 1995b), and fine-scale filamentary structure in corona] sti earners (Woo et al. 1995a). Source surface magnetic field maps (Hoeksema and Scherrer 1986) have played a key role in

understanding the coronal results deduced from these measurements, but in this paper wc will compare the ranging measurements with the more relevant white-light measurements (Woo 1996c). Fortunately, white-light measurements were available from the HA() Mauna Loa Solar Observatory Mk 111 K-coronameter (Sime et al., 1990) at the time of the Ulysses measurements.

Shown in Fig. 1 arc the K-coronameter synoptic maps (courtesy of J. Burkepile at HAO) based on polarized brightness pB measurements on the west limb at heights of 1.36 R_o and 1.74 R. for Barrington rotations 1845 and 1846. During this time, Ulysses ranging measurements took place simultaneously off the west limb, but at higher altitudes. The black dots on the K-coronameter maps represent the closest approach points of the Ulysses radio path mapped back to the Sun during the period of DOY 241–249. The corresponding time series of the Ulysses ranging measurements of time delay sampled once every 10 reins is displayed in Fig. 2a in reverse time order for the convenience of comparison with the K-coronameter maps. The majority of the contribution to path-integrated density observed by ranging measurements comes from that portion of the raypath that is subtended by an angle of approximately 60° about the point of closest approach point as measured from Sun center. The white-light measurements in Fig. 1 show that the Ulysses radio measurements probed an equatorial coronal hole located in a region of low solar activity during the period of DOY 241-248. Corresponding radial distances arc marked at the top of Fig. 2a showing that the measurements took place in the range of 23-42 R_o.

We have multiplied the ranging measurements by $(1\,\mathrm{AIJ}/R)^{1.42}$, where R is heliocentric distance in AU, in order to remove the radial dependence, and displayed the results in Fig. 2b. Normalization to 1 AU is for the convenience of comparing measurements at different radial distances, and is not meant to imply that the ranging measurements can be extrapolated to 1 AU. The remaining background density has been removed with a quadratic fit, and the results are shown in Fig. 2c. Although the removed

R-142 radial dependence is that determined from the Ulysses measurements off the west limb of the Sun by Bird et al. (1994), the results in Fig. 2c do not depend much on the actual radial dependence used.

The ranging system has a point-to-point variation in time delay of less than 1 ns and a day-to-day variation of less than about 3-4 ns (private communication J.R. Smith). Thus, although there are gaps in the data, the variation in path-integrated density in Fig. 2a is real, and the systematic variation is suggestive of plume structures, for which six have been identified and labeled, Although the profiles of these structures look similar to those of coronal streamers, they are not only fainter but are distinguished by the fact that, unlike the case of coronal streamers, the associated small-scale structure is conspicuously smaller, i.e. $\Delta n/n$ is small (Woo et al. 1995b). Supporting evidence for plume structures is provided by comparing these ranging results with white-light coronagraph measurements of polar plumes made by Spartan 201-01 (Fisher and Guhathakurta 1995), and this is discussed in the next section.

3. PLUMES

Like in situ plasma measurements, ranging cannot unambiguously distinguish spatial and temporal variations. The major advantage of white-light images is that they clearly show the approximately radially expanding plumes, and provide information on the radial and latitudinal variations of path-integrated density. Although longitudinal variations cannot be observed with eclipse measurements, they can with a coronagraph using a sequence of images as the Sun rotates. However, since the sampling rate of these images is often low, the spatial resolution is generally rc latively coarse.

The ranging results in Figs. 2b and 2c can be compared with Figs. 2a and 2b of Fisher and Guhathakurta (1995) showing the latitudinal profiles at fixed heights in the corona of polarized brightness pB and polarized brightness minus fit observed by the Spartan white-light coronagraph at 2 R. in the north polar coronal hole. W hereas the Spartan

measurements represent latitudinal profiles of path-integrated density across polar coronal plumes imaged at the same time —- and hence variations in a direction approximately transverse to the plumes — the ranging measurements represent longitudinal profiles of path-integrated density obtained as the quasi-stationary plumes rotate across and in a direction parallel to the radio path. In spite of these differences, the ranging profiles in Figs. 2b and 2c bear striking resemblance to the white-light profiles in Figs. 2a and 2b of Fisher and Guhathakurta (1995), respectively.

The six identified plumes in Fig. 2c occur over a period of about 6.5 clays. For a 27-day solar rotation period, this corresponds to 6 plumes over an angular range of 87°, a frequency that is similar to the six plumes observed over 80° in the Spartan white-light measurements over the north polar coronal hole. As in the case of white-light measurements, the variation in path-integrated density in the ranging measurements across the plumes amounts to about ±10% of the ambient value of the coronal hole. This similarity in contrast — despite the large differences in coronal heights at which the ranging and white-light measurements took place —- is consistent with the fact that in the inner corona the radial dependencies of both dense structures and ambient coronal hole based on observation (Fisher and Guhathakurta 1995) and modeling (Habbal et al. 1995) are similar. Comparison of the widths of the rays deduced from ranging measurements with those from the Spartan white-light measurements will be ambiguous because of differences in observation geometry. Nevertheless, for the three better observed plumes in Fig. 2c (plumes 3,4 and 6), the full widths at half maximum arc a couple of degrees, consistent with those of polar plumes in the plane of the sky deduced from the Spartan measurements, and consistent with the notion that plumes are approximately radially expanding. The similarity in latitudinal (white-light) and longitudinal (ranging) profiles of plumes across a coronal hole also supports the fact that the plumes are dissociated with the intergranular network since the network is circularly symmetric.

Because plumes are faint and low-contrast structures, high sensitivity, wide dynamic range, high precision and high stability are measurement features that are necessary for detecting them. in this regard, ranging measurements, which were developed for the precise navigation of planetary spacecraft, are superior to white-light measurements. While the detection of plumes in low-latitude coronal holes has been possible with ranging measurements because the measurement uncertainties are significantly smaller than the variations across the plume structures as evident in Fig. 2, this has not been the case with white-light measurements (Guhathakurta and Fisher, 1995).

Multiple-station intensity scintillation measurements — also carried out with radio sources as they pass behind the corona, and known as IPS for interplanetary scintillation — complement the path-integrated measurements of density by providing estimates of solar wind velocity (Dennison and Hewish 1967; Coles 1993). IPS measurements can yield some information on the variation of solar wind velocity across the plumes. Unfortunately, unlike path-integrated density, there are no velocity imaging measurements to unambiguously show spatial structure in the corona. Moreover, the solar wind velocity estimates deduced from IPS measurements are not as easy to interpret as path-integrated density measurements. First, the velocity measurements are deduced estimates that are dependent on the distribution of solar wind velocity along the raypath — and hence solar wind models. Second, the temporal resolution of IPS measurements is limited by the minimum observation time needed to obtain accurate estimates of velocity, leading to a spatial resolution for rotating coronal structures that is generally significantly coarser than that of ranging or Doppler measurements. '1'bird, unlike ranging measurements made with the NASA Deep Space Network (DSN), continuous IPS measurements are precluded by the absence of a worldwide network of IPS observatories, thus making it difficult to observe large-scale structures such as low-latitude plumes. In spite of these disadvantages, velocity estimates deduced from IPS measurements inside 12 R. using the VLA in 1983 (Armstrong et al. 1986), and obtained in a low-latitude coronal hole over an interval of

about 8 hours (corresponding to an angular extent in longitude of 4.40), show an apparent systematic variation in solar wind speed [see Fig. 2 of Woo (1995)], Although the absolute wind speed estimates are dependent on modeling (Grall 1996), the relative changes are less dependent, and the ±10% variation could represent the variation across a coronal plume.

4. DISCUSSION AND CONCLUSIONS

The search for plumes in ranging measurements is an outgrowth of the advances in our knowledge of structures in the corona, and progress in our understanding of ranging measurements and their relationship to white-light measurements, Although ranging measurements observe only one point of the white-light images, the extent to which these two types of measurements complement each other is significant. White-light images play a crucial role in identifying spatial structures, While white-light images provide latitudinal profiles, ranging provides longitudinal profiles of path-integrated density. The high sampling rates available with ranging or Doppler measurements make it possible to investigate structures that are much finer than those observed in white-light (Woo et al. 1995a). However, large-scale structures such as plumes require observations that are continuous or near-continuous for many days, which is oniy possible with a worldwide tracking network like the NASA DSN. Since ranging and Doppler measurements in the past have generally been of short duration, small-scale structures were the first to be recognized, and only now have plumes been identified. This is the opposite of the situation with white-light measurements, where large-scale structures such as plumes were first revealed, and smaller structures only revealed when spatial resolution improved.

Fortuitously, the extended Ulysses ranging measurements of the equatorial region took place at a time in the solar cycle when the warp of the heliospheric current sheet was large enough that a major equatorial coronal hole had formed. The high sensitivity, wide dynamic range, high stability, high precision, and long duration features of ranging

measurements have made it possible to detect plumes in this coronal hole, while the similarity between the longitudinal profile obtained from the Ulysses ranging measurements and the latitudinal profile from the Spartan white-light measurements across polar plumes has made it possible to identify them,

The results of this paper, together with EUV measurements of the inner corona (Wang et al. 1995), indicate that plumes arc not exclusive to polar regions, but appear to be intrinsic to open magnetic field regions at any latitude. Like white-light measurements of polar plumes in the inner corona, ranging measurements show a variation in path-integrated density of ±10% across the plumes, and are consistent with the notion that the plumes are approximately radially expanding. Measurements of solar wind speed deduced from IPS measurements over a low-latitude coronal hole suggest that the solar wind speed inside $12\,R_{\odot}$ may vary by ±1 O% across the plumes.

The detection of plumes at low latitudes reinforces the picture of a corona that is pervaded by raylike structures having a wide range of scale sizes, and further demonstrates the unique role of radio propagation measurements in characterizing the plasma properties — electron density, solar wind velocity, and magnetic field — of the structures in a region that has not been accessible to direct measurements. This region is also important because, unlike beyond 0.3 AU where only vestiges arc observed (Thieme et al. 1990; McComas et al. 1995), the structures arc more pristine and less evolved near the **Sun.** The ubiquity of coronal structures and the experience with radio propagation measurements also point to the value of imaging the corona when in situ plasma measurements will finally be made by a mission to the Sun such as Solar Probe (Feldman et al. 1989). Such imaging is crucial not only for a definitive understanding of the role of the structures in coronal heating and acceleration of the solar wind, but also for placing the in situ plasma measurements into context.

1(is a pleasure to acknowledge the outstanding support received from the Ulysses Project and the NASA DSN. We are especially grateful to J. Armstrong for valuable discussions and comments on this paper, C. Chang for programming and data processing, and to S. Asmar, P. Eshe, and R. Horton of the Radio Science Support Team. Long duration tracking of Ulysses by the NASA DSN was essential for the results of this paper, and wc are indebted to J. Brenkle for his efforts in arranging it. We also thank J.R. Smith for discussions about the ranging, measurements, and J. Burkepile for kindly providing the HAO K-coronametcr synoptic maps, This paper describes research carried out at the Jet Propulsion Laboratory, California Institute of Technology, under a contract with the National Aeronautics and Space Administration, and presents results of a research project partially funded by the Deutsche Agentur fur Raumfahrtanglegenheiten (DARA) GmbH under the contracts50ON9104 and 50 ON 9401.

REFERENCES

Ahmad, I.A., & Withbroe, G.L. 1977, Solar Phys., 53, 397

Ahmad, I.A., & Webb, D.F. 1978, Solar Phys., 58, 323

Abbot, C.G. 1900, Ap. J., 12,69

Armstrong, J. W., Coles, W. A., Kojima, M., & Rickett, B.J. in The Sun and the Heliosphere in Three Dimensions, cd. R.G. Marsden (Dordrecht: D. Reidel), 59

Bird, M.]{., & Edenhofer, P. 1990, in Physics of the Inner Heliosphere 1, eds. R. Schwenn, & E. Marsch (Berlin: Springer), 13

Bird, M. K., Volland, H., Pätzold, M., Edenhofer, P., Asmar, S. W., & Brenkle, J.P. 1994, Ap. J., 426, 373

Bohlin, J. D., Sheeley, N. R., Jr., & Touscy, R. 1975, in Space Research XV, ed. M.J. Rycroft (Berlin: Akademie),651

Coles, W.A. 1993, in Wave Propagation in Random Media (Scintillation), eds. V.I. Tatarskii, A. Ishimaru, & V.U. Zavorotny (Bellingham: SPIE), 156

Dennison, P. A., & Hewish, A. 1967, Nature, 213, 343

Feldman, W. et al. 1989, Solar Probe Scientific Rationale and Mission Concept (J PI. Rept. D-6797)

Fisher, R., & Guhathakurta, M. 1995, Ap. J., 447, L139

Grail, R.R. 1995, PhD thesis, University of California, San Diego

Guhathakurta, M., & Fisher, R. 1995, Geophys. Rcs. Lett., 22, 1841

Habbal, S.R. 1992, Ann. Geophys., 10, 34

Habbal, S. R., Esser, R., Guhathakurta, M., & Fisher, R.R. 1995, Geophys. Res. Lett., 22, 1465

Hoeksema, J. T., & Scherrer, P.H. 1986 The Solar Magnetic Field — 1976 through 1985 (Rep. UAG-94, World Data Cent. A for SOI. Terr. Phys.)

Koutchmy, S. 1977, Solar Phys., 51, 399

Koutchmy, S., & et al. 1994, Astron. Astrophys., 281, 249

McComas, D. J., Barraclough, B.L., Gosling, J. T., Hammond, C, M., Phillips, J.],., Neugebauer, M., Balogh, A., & Forsyth, R.J. 1995, J. Gophys. Res., 100, 19893

Newkirk, Jr., G., & Harvey, J. 1968 Solar Phys., 3, 321

Saito, K. 1965, Publ. Astron. Sot. Japan, 17, 1

Sime, D.G. et al. 1986, The White Light Solar Corona: An Atlas of 1985 K-Coronameter Synoptic Charts December 1984–December 1985 (NCAR/TN-274 + STR)

Thieme, K. M., Marsch, E., & Schwenn, R. 1990, Ann. Geophys., 8, 713

van de Hulst, H.C. 1950, Bull. Astron. Inst. Neth., 11, 150

Velli, M., Habbal, S. R., & Esser, R. 1994, Space Sci. Rev, 70, 391

Walker, Jr., A. B.C., DeForest, C. E., Hoover, R. B., & Barbee, Jr., T.W. 1993, Solar Phys., 148, 239

Wang, Y.-M. 1994, Ap. J., 435, L153

Wang, Y.-M., & Sheeley, Jr., N.R. 1995, Ap. J., 446, L51

Widing, K. G., & Feldman, U. 1992, Ap. J., 392, 715

Woo, R. 1995, Geophys. Res. Lett. 22, 1393

Woo, R. 1996a, Nature, 369, 321

Woo, R. 1996b, in Proceedings of Solar Wind Eight, edited by D. Winterhalter, J. Gosling, S. R. Habbal, W. Kurth, and M. Neugebauer (New York: AIP)

Woo, R. 1996c, Ap. J., 458,

Woo, R., Armstrong, J. W., Bird, M. K., & Pätzold, M. 1995a, Ap. J., 449, L91

Woo, R., Armstrong, J. W., Bird, M, K., & Pätzold, M. 1995b, Geophys. Res. Lett., 22, 329

LIST OF FIGURES

Fig. 1 HAO Mauna Loa Solar Observatory Mk 111 K-coronameter synoptic maps (courtesy of J. Burkepile) based on polarized brightness pB measurements on the west limb at heights of 1.36 R. and 1.74 R_o. The black dots on the maps, which represent the closest approach points of the Ulysses radio measurements in Fig. 2 mapped back to the Sun, indicate that during the period of DOY 24 1–249 Ulysses probed an equatorial hole.

Fig. 2 Time series of (a) time delay $\Delta\tau$ sampled once every 10 reins. by Ulysses ranging measurements, (b) normalized time delay with radial dependence removed from (a) by multiplying by (1 AU/R--l $^{.42}$, and (c) normalized time delay in (b) with quadratic fit removed. The time series in (b) and (c) arc similar to those of polar coronal plumes from the Spartan white-light pictures and shown in Figs. 2a and 2b of Fisher and Guhathakurta (1995), respectively.

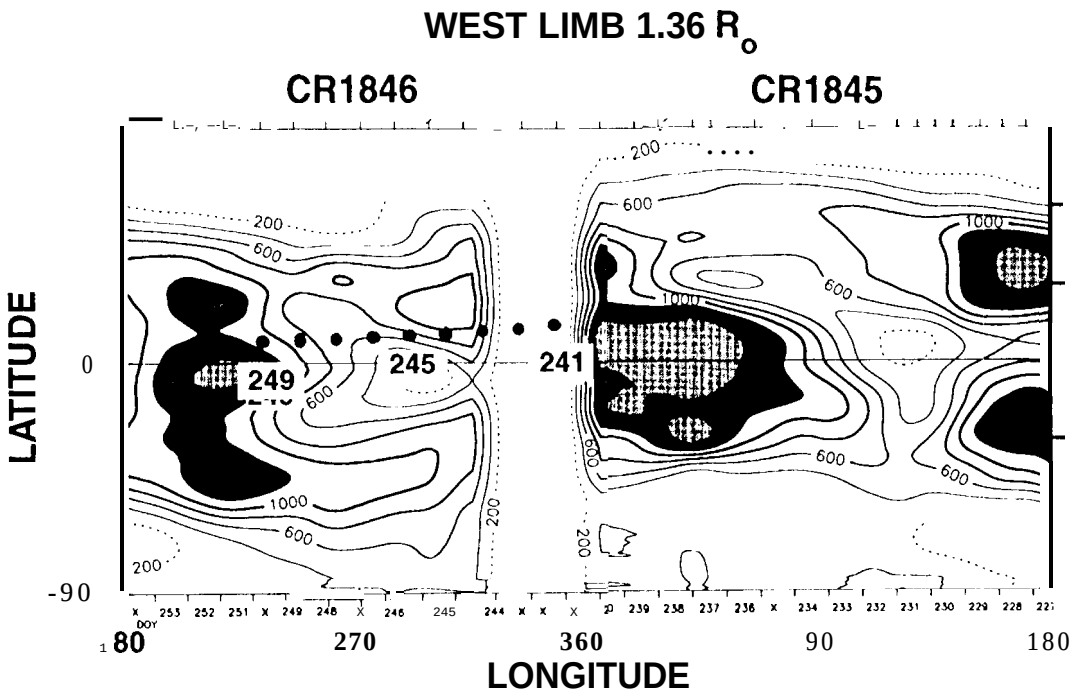
WEST LIMB 1.36 R$_o$
CR1846
CR1845
LATITUDE
0
-90
249
245
241
200
600
1000
DOY
180
270
360
90
180
LONGITUDE

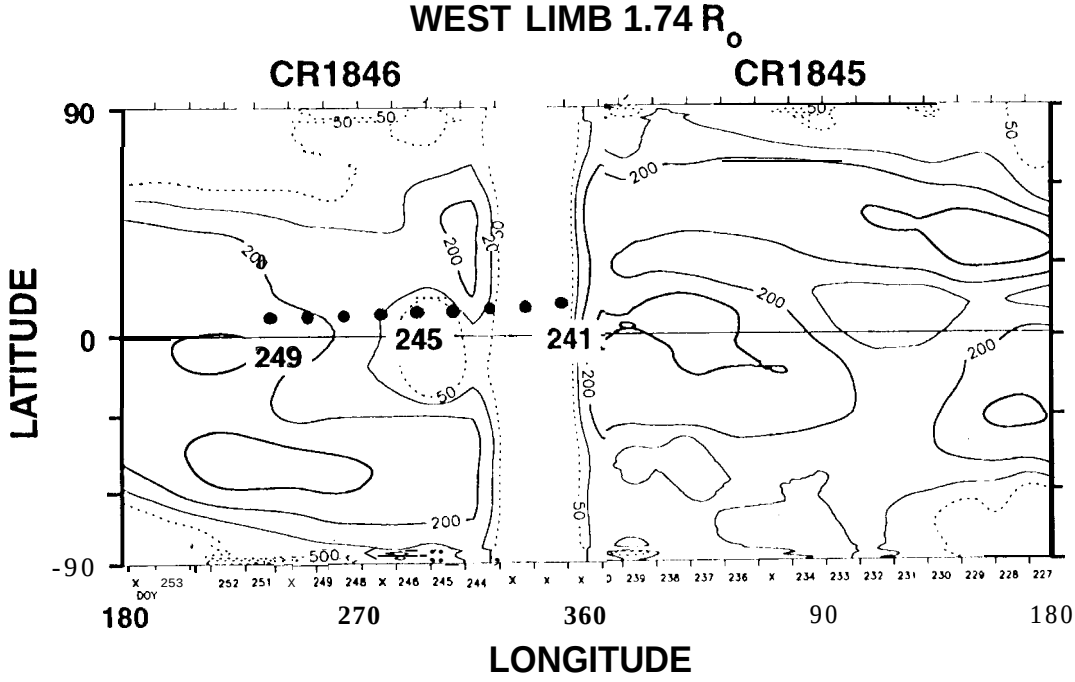
WEST LIMB 1.74 R$_o$
CR1846
CR1845
LATITUDE
90
0
-90
249
245
241
50
200
500
DOY
180
270
360
90
180
LONGITUDE

Fig 1

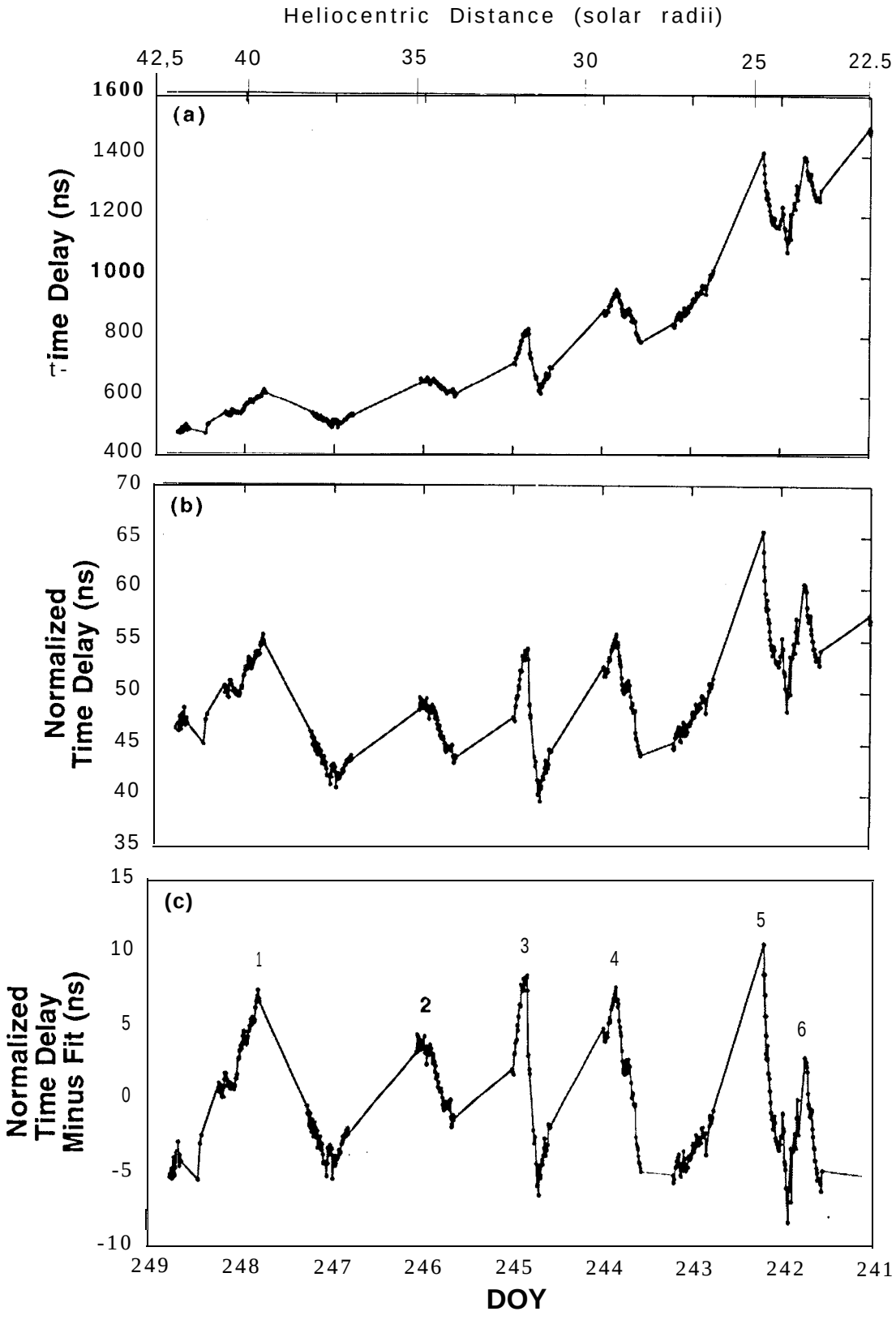
Heliocentric Distance (solar radii)
42,5
40
35
30
25
22.5
1600
1400
1200
1000
800
600
400
t- ime Delay (ns)
(a)
70
65
60
55
50
45
40
35
Normalized Time Delay (ns)
(b)
15
10
5
0
-5
-10
Normalized Time Delay Minus Fit (ns)
(c)
1
2
3
4
5
6
249
248
247
246
245
244
243
242
241
DOY